International Journal of Nanoelectronics and Materials
*Volume 16 (Special Issue) December 2023* [9-16]

# Design Simulation of Circular Photonic Crystal Structures for the Development of Biomedical Sensor Based on Finite Difference Method

Teguh Puja Negara[1,2], Hendradi Hardhienata[1], Irzaman[1], and Husin Alatas[1,*]

[1]Theoretical Physics Division, Department of Physics, Faculty of Mathematics and Natural Science, IPB University, Bogor, Indonesia
[2]Department of Computer Science, Faculty of Mathematic and Natural Science, Universitas Pakuan, Bogor, Indonesia

**ABSTRACT**

*Optical analysis of a circular photonic crystal structure consisting of a metal-dielectric layer and a defect layer sandwiched between two dielectric layers has been carried out using the Finite Difference Frequency Domain (FDFD) method and the Finite Difference Time Domain (FDTD) method. The FDTD method can describe the propagation of electromagnetic waves on the structure at any time, while the FDFD method can describe the characteristics of the wave interaction with the structure in a steady state. We observed strong resonances at certain wavelengths when using three different dielectric materials:* $BaTiO_3$, $ZnSe$, *and* $ZnTe$. *The simulation results show a change in the resonance peak in the sensing material in the form of normal blood and blood-containing glucose in the defect layer for concentration:* $0 - 350\ mg/dL$. *The use of three different dielectric materials produces different sensitivity values. The highest sensitivity value when using* $ZnSe$ *material that produces a sensitivity value of* $26.6063$ *at the refractive index intervals* $2.499 - 2.72$. *The simulation results can be used to build biomedical sensors that measure blood sugar levels.*

**Keywords:** Circular photonic crystal, finite difference time domain, finite difference frequency domain, biomedical sensor

## 1. INTRODUCTION

The simulation of electromagnetic wave propagation in photonic crystals has been intensely investigated by researchers owing to their interesting applications in optics, such as waveguides [1], solar cells [2], and sensors [3]. The emerging optical characteristics of photonic crystals, namely changes in the transmittance peak [4] or shifts in the transmittance band [5] owing to changes in the material's refractive index, have been directed toward optical biosensors. A computational method was developed to design structures with adjustable materials and thicknesses and to analyze the propagation of electromagnetic waves in these structures. Several numerical methods have been used to simulate the propagation of electromagnetic waves in photonic crystal structures, namely the finite-difference time-domain (FDTD) and finite-difference frequency-domain (FDFD) methods. The FDTD method can describe the propagation of electromagnetic waves on a structure at any time [6], whereas the FDFD method can describe the characteristics of wave interactions on a structure in a steady state [7]. In previous studies, the FDTD and FDFD methods were carried out separately on layered photonic crystal structures [8], rod photonic crystals [9], and grating photonic crystals [10].

The proposed photonic crystal structure is a circular photonic crystal with a metal-dielectric layer accompanied by channels to investigate the pattern of the transmittance wave when there is a change in the analyte being sensed. Simulations were performed using the FDTD and FDFD methods simultaneously to analyze the interaction of waves with circular photonic crystal structures involving second-order differential equations. Previous research has been conducted

* Corresponding authors: alatas@apps.ipb.ac.id

on the propagation of electromagnetic waves in layered photonic crystal structures using analytical methods to build concentration sensor devices [11]. The focus of the simulations carried out in this research is the analysis of changes in the peak transmittance caused by changes in the analyte's refractive index in the form of blood, which varies based on the sugar content. The results of this research can be applied to optical-based biomedical sensors, which is a breakthrough considering that sensor devices in the medical field are generally chemical-based [12].

## 2. MATERIAL AND METHODS

### 2.1 Finite Difference Method

Finite Difference Time Domain (FDTD) is a method that uses an approach to the time and space domains. The FDTD method was first introduced by Yee in 1966 to analyze electromagnetic fields [13]. The FDTD method alternately describes the propagation of electric and magnetic fields in spatial coordinates at any time, at a single frequency. Optical phenomena, such as diffraction, scattering, reflection, and absorption, can be clearly described when an electromagnetic field interacts with a structure at any time. The finite-difference frequency-domain (FDFD) method is a numerical solution for electromagnetic and acoustic problems. The FDFD method can solve differential equations by forming eigenvalue equations to obtain field equations in the space, frequency, and wavelength domains [14]. The FDFD method describes the propagation of the electric and magnetic fields in spatial coordinates at each frequency in a steady state.

In FDTD, the electric and magnetic field discretization in the domain for the transverse magnetic (TM) mode can be written as follows:

$$H_{z(i,j)}^{n+\frac{1}{2}} = H_{z(i,j)}^{n-\frac{1}{2}} + \frac{\Delta t}{\mu \Delta y}\left(E_{x(i,j+\frac{1}{2})}^{n} - E_{x(i,j-\frac{1}{2})}^{n}\right) - \frac{\Delta t}{\mu \Delta x}\left(E_{y(i+\frac{1}{2},j)}^{n} - E_{y(i-\frac{1}{2},j)}^{n}\right) \tag{1}$$

$$E_{x(i,j)}^{n+1} = E_{x(i,j)}^{n} + \frac{\Delta t}{\varepsilon \Delta y}\left(H_{z(i,j+\frac{1}{2})}^{n+\frac{1}{2}} - H_{z(i,j-\frac{1}{2})}^{n+\frac{1}{2}}\right) \tag{2}$$

$$E_{y(i,j)}^{n+1} = E_{y(i,j)}^{n} + \frac{\Delta t}{\varepsilon \Delta x}\left(H_{z(i+\frac{1}{2},j)}^{n+\frac{1}{2}} - H_{z(i-\frac{1}{2},j)}^{n+\frac{1}{2}}\right) \tag{3}$$

Meanwhile, in FDFD, the discretization of the electric and magnetic fields in the frequency domain for the transverse magnetic (TM) mode can be written as follows:

$$\begin{pmatrix} 0 & -\boldsymbol{D}_z^H & \boldsymbol{D}_y^H \\ \boldsymbol{D}_z^H & 0 & -\boldsymbol{D}_x^H \\ -\boldsymbol{D}_y^H & \boldsymbol{D}_x^H & 0 \end{pmatrix} \begin{pmatrix} 0 \\ 0 \\ H_z \end{pmatrix} = \begin{pmatrix} \varepsilon_{xx} & 0 & 0 \\ \boldsymbol{D}_z^H & \varepsilon_{yy} & 0 \\ 0 & 0 & \varepsilon_{zz} \end{pmatrix} \begin{pmatrix} E_x \\ E_y \\ 0 \end{pmatrix} \tag{4}$$

The electric and magnetic fields that propagate in the computational space are limited by an imaginary medium that absorbs waves called Boundary Conditions. The commonly used boundary condition is the perfectly matched layer (PML) [15]. The field that passes through the structure (transmittance) and the field that is reflected (reflectance) can be calculated using the following equations:

$$T = |S_{trn}|^2 \left(\frac{k_{trn}\varepsilon_{r,trn}}{k_{inc}\varepsilon_{r,inc}}\right) \tag{5}$$

Where $S_{trn}$ and $k_{trn}$is are the transmittance coefficient and the vector of the transmittance wavenumber, $k_{inc}$, and $\varepsilon_{r,trn}$ and $\varepsilon_{r,inc}$, are the relative permittivity of the material at the transmittance limit and the relative permittivity of the material at the source, respectively.

The sensor calculation was based on the change in the transmittance peak with respect to the change in the refractive index of the material. If there is a change in the transmittance peak due to a change in the refractive index of the material, the sensitivity calculation is calculated as follows:

$$S = \frac{dT_p}{dn_d} \tag{6}$$

Where $T_p$ is the value of the peak transmittance and $n_d$ is the refractive index of the sensing material (analyte).

## 2.2 Design Structure

The corresponding device model is illustrated in Figure 1. The periodic metal-dielectric cylinder is formed with parameters and sizes according to the design that has been made, and we considered a periodic metal-dielectric cylinder with one defect cylinder of refractive index $n$ in the middle, which is considered as an analyte. The system is illuminated by a continuous electromagnetic field from the center side, which is perfectly guided inside the dielectric cylinder by the channel. The dielectric layers used were $BaTiO_3$ with a refractive index 2.472, $ZnSe$ with a refractive index 2.6123, and $ZnTe$ with a refractive index 3.0631, which can be compared to the optical response to changes in the refractive index of the analyte. The metal layer was gold and had refractive indices following the Drude-Lorentz formulation [16].

$$n(\lambda) = \sqrt{\varepsilon(\lambda)} = \sqrt{1 - \frac{\lambda^2 \lambda_c}{{\lambda_p}^2(\lambda_c + i\lambda)}} \tag{7}$$

where $\lambda_p$ is the plasma wavelength, and $\lambda_c$ is the collision wavelength. The values of $\lambda_p$ and $\lambda_c$ for gold were $1.6826 \times 10^{-7}m$ and $8.9342 \times 10^{-6}m$ respectively. The thicknesses of the dielectric and gold layers were the same, namely 400 $nm$. The wavelength is given in the visible light range of : $\lambda_0 = 400 - 700\ nm$ or the frequency range in THz is $f_0 = 0.4 - 0.7\ THz$. The use of frequencies in the terahertz range is a very special and interesting part of the electromagnetic (EM) spectrum. In the simulation, we used $200 \times 200$ meshes, where each mesh had dimensions of $dx = dy = 20\ nm$. For the time step we set $1.67 \times 10^{-14}s$.

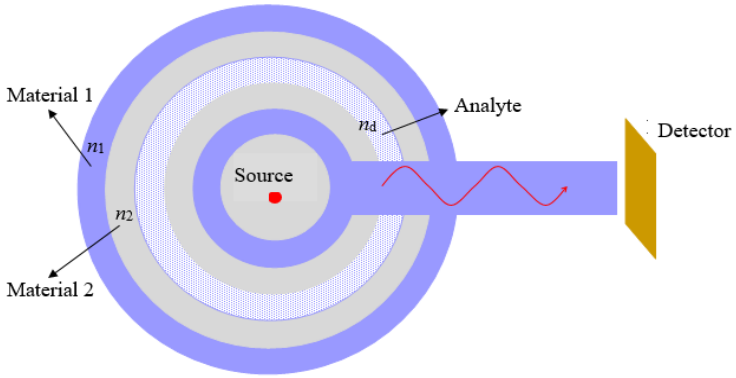


**Figure 1.** Metal-dielectric cylinder structure.

Transmittance analysis is based on changes in the transmittance profile with variation in the refractive index value of the analyte. Based on ref [17], the refractive index of blood is approximately 1.341. In the presence of glucose in the blood, the refractive index of the blood changes according to the concentration of glucose in the blood, according to the table obtained from ref [18].

**Table 1** Refractive index for blood

| Glucose concentration in $mg/dL$ | Refractive index |
|---|---|
| 0 | 1.333 |
| 50 | 1.59950 |
| 100 | 1.77718 |
| 150 | 1.99929 |
| 200 | 2.16135 |
| 250 | 2.32469 |
| 300 | 2.71999 |
| 350 | 2.98384 |
| 400 | 3.27384 |

## 3. RESULTS AND DISCUSSION

The sketch model is shown in Fig. 1 which is homogeneous in the z-direction. In this simulation. We used seven layers of dielectric and metal periodically circularly, with a defect in the middle. The resulting electric field distribution shows that the field cannot penetrate the metal layer, spreads only in the channels, and is distributed in the dielectric layer (Fig. 2). Waves traveling through channels are guided waves. At time $6.68 \times 10^{-12} s$, the wave reaches a steady state, and the transmittance is calculated based on the wave value at the end of the channel against the input waveform.

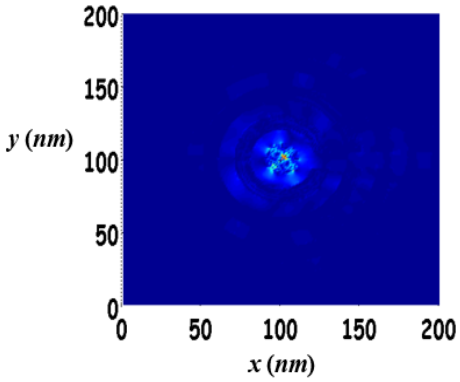


**Figure 2.** Metal-dielectric cylinder structure.

One of the optical responses that can be analyzed in the development of optical devices is the transmission profile. The transmittance curve for the proposed structure shows the existence of a resonance mode at several wavelengths at different positions according to the selection of the dielectric material used. For the simulation results in Figure 3, the highest resonance is at a wavelength $432\ nm$ when using the dielectric material $BaTiO_3$, is on the wavelength $455\ nm$ when using the dielectric material $ZnSe$, and is on the wavelength $609\ nm$ when using the

dielectric material $ZnTe$. The difference in the position of the resonance mode is based on the difference in the refractive indices of the two photonic crystal layers.

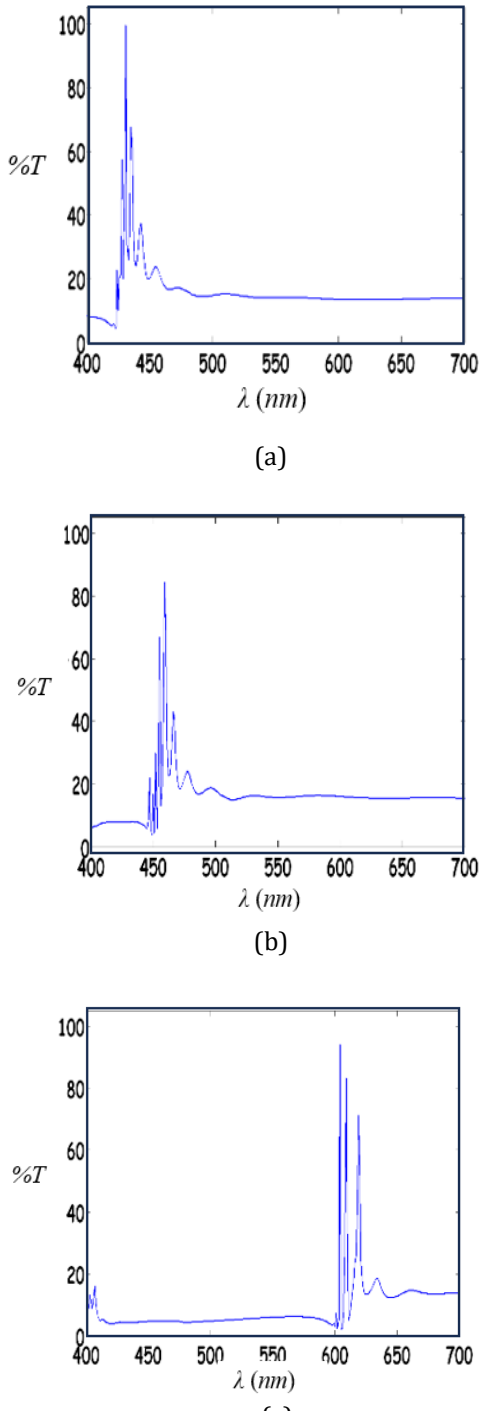


**Figure 3.** Transmittance profiles for different dielectric materials: (a) $BaTiO_3$, (b) $ZnSe$, (c) $ZnTe$.

Changes in the refractive index of the test material cause changes in the resonance peak, which can be developed on the sensor. For the sensing material, the refractive index 1.341. Simulation results for changes in one of the resonance peaks for normal blood and glucose-containing blood sensing materials at concentrations of 50 $mg/dL$ ($n = 1.59950$), 150 $mg/dL$ ($n = 1.99929$), and 250 $mg/dL$ ($n = 2.32469$) in the defect layer are shown in figure 4. The resonance changes

significantly at a wavelength 431 $nm$ for the material $BaTiO_3$, is on the wavelength 455 $nm$ for material $ZnSe$, and 604 $nm$ for material $ZnTe$.

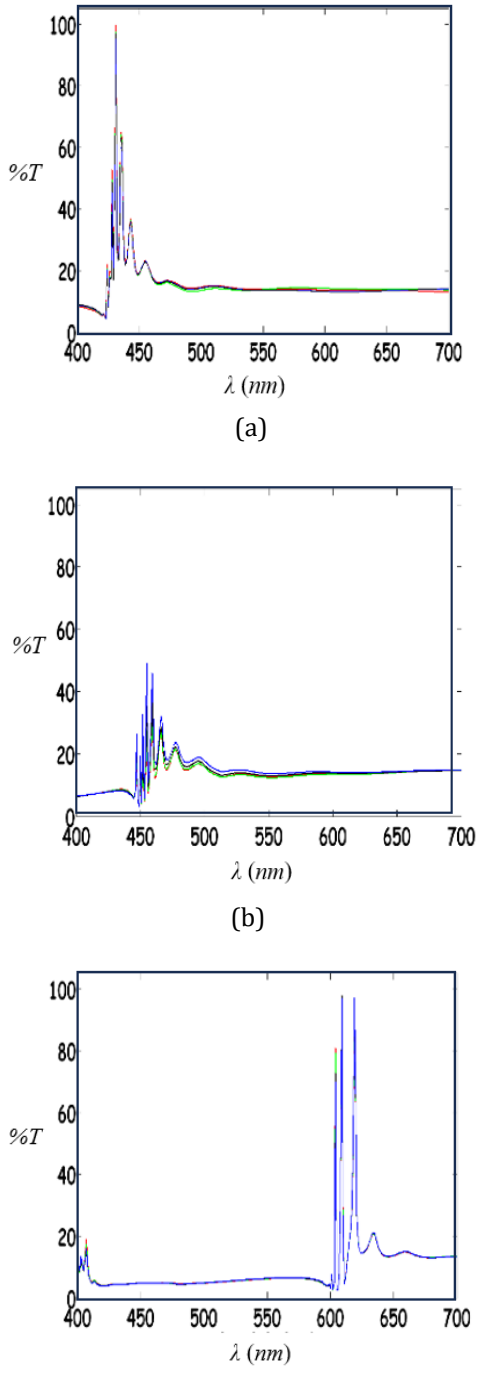


**Figure 4.** Transmittance profiles for different dielectric material with a change in the refractive index of analytes: (a) $BaTiO_3$, (b) $ZnSe$, (c) $ZnTe$.

The response of changes in the transmission peaks to changes in the refractive index of analytes corresponding to changes in blood sugar levels is shown in Figure 5. In the refractive index range of $1.333 - 2.7199$, the transmittance value changes nonlinearly for the material: $BaTiO_3$, $ZnSe$, and $ZnTe$. However, within a certain range of the refractive indices, a linear range was obtained for these materials. For the dielectric material $BaTiO_3$, a linear response is produced over a range of refractive index $1.777 - 1.999$ at a wavelength 431 $nm$ with a sensitivity 21.982. For the

dielectric material $ZnSe$, a linear response is produced over a range of refractive indices $2.499 - 2.72$ with a wavelength $459\ nm$ and a sensitivity 26.6063. For the dielectric material $ZnTe$, a linear response was produced over a range of refractive index $1.999 - 2.161$. on a wavelength $604\ nm$ with a sensitivity 11.2963. These results are important for selecting a dielectric material for a given structure to develop sensors that can measure sugar content over a specific wavelength range.

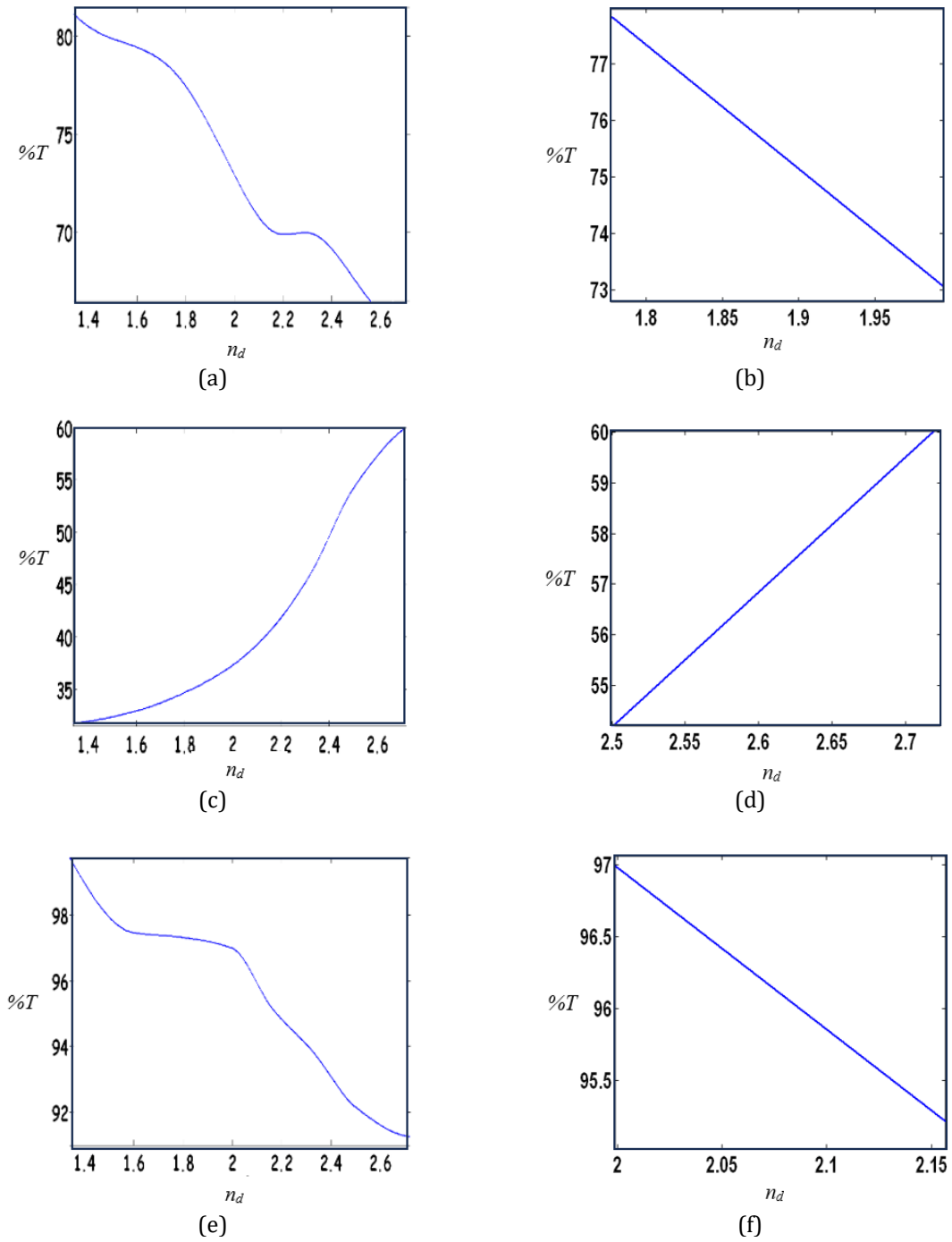


**Figure 5.** Transmittance response to changes in the refractive index of glucose-containing blood for different dielectric materials: (a) $BaTiO_3$, (b) $ZnSe$, (c) $ZnTe$.

## 4. CONCLUSION

The electromagnetic wave propagation on circular photonic crystal structures with metal-dielectric layers was simulated using the FDTD and FDFD methods. The simulation results show that wave propagation occurred through the dielectric channel. The differences in the dielectric materials used are $BaTiO_3$, $ZnSe$ and $ZnTe$ produce an optical response, namely, the transmittance at different wavelength positions. Changes in the refractive index of the sensing material cause changes in the transmittance peak at certain wavelengths. The simulation results for material sensing in the form of blood containing glucose produced a transmittance peak that changed linearly in a certain wavelength range according to the dielectric material used. The highest sensitivity value when using $ZnSe$ material that produces a sensitivity value 26.6063 at refractive index intervals $2.499 - 2.72$

## REFERENCES


[1] Wei, E, I, S., Xian L, W., Zhi, X, H., and Ming, S, C., *Progress in Electromagnetics Research* B. vol. **13** (2009) pp. 237-256

[2] Dario, C., Carmen, M, R., David, D., Sergio, G., Edgardo, S., Jean, J, S., and Ludovic, E., *Optics Express*. vol **24** issue18 (2016) pp. A1201–A1209

[3] Parisa, E., Fateme., S., *Sensing and Imaging*. vol **24** issue 1 (2023) pp.1-19

[4] Alatas, H., Hasan, M., Hendradi, H., Alexander, I., Tjia, M, O., *Jpn. J. Appl. Phys* . vol **45** issue 8B (2006) pp. 6754- 6758

[5] Xiangxian, W., Xiaoxiong, W., Jiankai, W., Zhiyuan, P., Hua,Y., Yunping, Q., *Sensors*. vol **19** issue 5 (2019) pp. 1-10

[6] Theodoros., *Mathematical Problems in Engineering*. vol. **9247978** (2017) pp. 1–8

[7] Jianming, W., Xinbo, H., Bing, W., Xianglin, L., *Journal of Electrical and Electronic Engineering***.** vol **9** issue 6 (2021) pp.186-193

[8] Hendradi, H., Teguh, P, N., Budi, S., Hasan, M., Husin, A., "*Photonic Pass-Band Characteristics of a One Dimensional Photonic Crystal with Two Defects at Omnidirectional Light Incident*," in Proc. International Conference on Mathematics and Natural Sciences (2006) pp. 907-910

[9] Adly, M, S., Teguh, P, N., Hendradi, H., Husin, A., 2019 *Komputasi*. vol **16** issue 2 2019 pp. 255-262

[10] Teguh, P, N., Garnadi, A, D., Nurdiati, S., Husin, A., 2014 *Optik* vol **125** (2014) pp 3134-3137

[11] Mamat R., Teguh, P, N., Hendradi, H., Irmansyah., Husin, A., "*Real-Time Optical Sensor Based on One Dimensional Photonic Crystals with Defects*," in IEEE Proc. of International Conference on Communication, Information, Instrumentation and Biomedical Engineering (2009) pp. 1-5

[12] Lillian, B, H., Najwa, L., Grace, E, C., Julie, A, P., and Michael, C, L., 2019 *Sensors*. vol **19** issue 11 (2019) pp. 1-25

[13] Kane, S, Y., *IEEE Transactions on Antennas and Propagation* vol **14** issue 3 (1996) pp. 302-307

[14] David, I., Care, M, P., *International Journal of Antennas and Propagation*. vol. **274063** (2014) pp. 1-9

[15] Jean, P, B., *Journal of Computational Physics* vol **114** issue 2 (1994) pp. 185-200

[16] Min, X., Chuanxing, T., Ming, C., Yu, C., Shijie, D., Fuwang, L., Hongchang, D., Houquan, L., and Libo, Y., *Sensors* vol **22** issue 15 pp. 1-10

[17] Mohamed, A, E., *AIMS Biophysics*. vol 8 issue 1 (2021) pp. 57-65

[18] Tadesse, W, G., Dabbu, S., *J. Pharm and Tech*. vol **12** issue 2 (2019) pp. 831-840